

# Effect of the oxygen balance on ignition and detonation properties of liquid explosive mixtures

M Genetier, A Osmont and G Baudin

CEA, DAM, GRAMAT, F-46500, Gramat, France

E-mail: antoine.osmont@cea.fr

**Abstract.** The objective is to compare the ignition and detonation properties of various liquid high explosives having negative up to positive oxygen balance (OB): nitromethane ( $OB < 0$ ), saccharose and hydrogen peroxide based mixture (quasi nil OB), hydrogen peroxide with more than 90% purity ( $OB > 0$ ). The decomposition kinetic rates and the equations of state (EOS) for the liquid mixtures and detonation products (DP) are the input data for a detonation model. EOS are theoretically determined using the Woolfolk *et al.* universal liquid polar shock law and thermochemical computations for DP. The decomposition kinetic rate laws are determined to reproduce the shock to detonation transition for the mixtures submitted to planar plate impacts. Such a model is not sufficient to compute open field explosions. The aerial overpressure is well reproduced in the first few microseconds, however, after it becomes worse at large expansion of the fireball and the impulse is underestimated. The problem of the DP EOS alone is that it takes only the detonation into account, the secondary combustion DP – air is not considered. To solve this problem a secondary combustion model has been developed to take the OB effect into account. The detonation model has been validated on planar plate impact experiments. The secondary combustion parameters were deduced from thermochemical computations. The whole model has been used to predict the effects of the oxygen balance on open air blast effects of spherical charges.

## 1. Introduction

The aim of this study is to compare the ignition and detonation properties of various liquid high explosives, one with a negative oxygen balance, another one with a quasi nil balance and a last one with a positive balance. The first one is nitromethane (NM). The second one is a solution of saccharose in hydrogen peroxide (HPS) to adjust the oxygen balance (OB) to the desire value (here zero). The third one is quasi pure hydrogen peroxide ( $H_2O_2/H_2O$ ) of positive OB.

The decomposition kinetic rates and the equations of state (EOS) for the liquid mixtures and detonation products (DP) are the input data for a detonation model (see section 2.2). EOS are theoretically determined using the universal liquid polar shock law and thermochemical computations for DP. The decomposition kinetic rate laws are determined to reproduce the shock to detonation transition (SDT) for the mixtures submitted to planar plate impacts (see section 2.1). It is well known that such a basic model, based on the simple EOS for DP leads to bad results for open field explosion. In such experiments, the overpressure signals are good in the first microseconds, however, after it becomes worse at large expansion of the fireball. As a consequence, the impulse is underestimated. The problem of the DP EOS alone is that it takes only the detonation into account, the secondary combustion (post-combustion) being not considered. As an example for TNT, the energy released during the post-combustion is twice the energy released during the detonation itself. To solve this



problem a secondary combustion model has been developed in the reference [1] to take the effect of oxygen balance on the secondary combustion of detonation products with air (see section 3) into account.

## 2. Detonation modeling

### 2.1. Experiments

The detonation behavior is explored through planar impacts realized with a powder gun of caliber 98 mm. The experimental setup used (figure 1) has been developed by Leal-Crouzet *et al.* [2] and is composed of a polyethylene vessel containing the high explosive impacted by a planar metallic projectile. The nature of the projectile and of the intermediary materials may change depending of the solicitation plan. Experiments are instrumented with piezoelectric pins to obtain the shock-to-detonation velocity, a VISAR measurement on the back side of the high explosive through a LiF window and a six-wave length pyrometer in the near UV - near IR range (see figure 2).

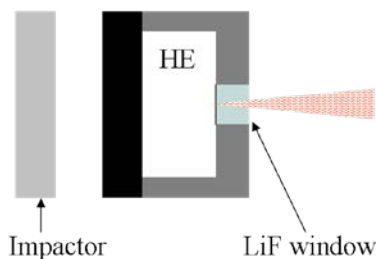


**Figure 1.** Experimental setup.



**Figure 2.** Photography of the experimental setup.

The four NM and the first HPS experimental setups are chosen to obtain a uniform pressure in the detonation products after shock to detonation transition. To obtain such detonation states, overdriven detonation are ignited inside the liquids by plate impact at high velocities. The second HPS one is chosen to exhibit the shock to detonation transition (SDT). This experiment will be used to calibrate the reaction rate following the method developed in [2]. Impactor and buffer plate thickness and velocities are given in the table 1.

**Table 1.** Experimental setup parameters

Exp.	HE	Impactor	Velocity – m/s	Buffer plate	Diagnostics
#1	HPS	15 mm Cu	2211	4 mm Al	Visar / DLI
#2	HPS	15 mm Cu	2111	4 mm Cu	Pyrometer
#3 & #4	NM	6 mm Ta/5 mm Al	2019	4 mm Al	Visar / DLI
#5 & #6	NM	5 mm Ta	2276	4 mm Ti/5 mm Al	Visar / DLI

### 2.2. Modeling

The reaction product-liquid mixture is described by the Helmholtz free energy proposed by Kerley *et al.* [3] expressed as:

$$\Psi(v, T, \lambda) = e + TS = (1 - \lambda_1)\Psi_{liq}(v, T) + \lambda_1\Psi_{DP}(v, T) + \lambda_2 Q_{PostComb}, \quad (1)$$

Where  $\lambda_1$  represent the SDT reaction coordinate and  $\lambda_2$  the secondary combustion reaction coordinate activated after SDT. Pressure and entropy are deduced from Helmholtz free energy by equations:

$$P = -\left(\frac{\partial \Psi}{\partial v}\right)_T, S = \left(\frac{\partial \Psi}{\partial T}\right)_v. \quad (2)$$

The liquids (liq) and the detonation products (DP) equations of state are expressed in a Mie-Gruneisen form:

$$\begin{aligned} e &= e_{ref}(\rho) + \frac{P - P_{ref}(\rho)}{\Gamma \rho} \\ T &= T_{ref}(\rho) + \frac{P - P_{ref}(\rho)}{\Gamma \rho C_V} \\ P_{ref} &= \rho^2 \frac{de_{ref}}{d\rho}. \end{aligned} \quad (3)$$

The liquids reference curves are the Cochran and Chan 0 K [4] isotherm:

$$P_{ref} = P_{ref}^{0K} = A_1 \left( \frac{\rho}{\rho_0} \right)^{E_1} - A_2 \left( \frac{\rho}{\rho_0} \right)^{E_2} \quad (4)$$

$$T_{ref}(\rho) = 0. \quad (5)$$

Parameters  $A_1$ ,  $A_2$ ,  $E_1$ , and  $E_2$  are computed using the relation proposed by Cochran and Chan to reproduce the Hugoniot curve  $D = c_0 + su$ . For HPS, the Hugoniot curve is deduced from universal form proposed by Woolfolk *et al.* [5] for liquids with a sound velocity deduced from the relation

$$c_0 = \frac{A + D.x^B}{1 + x^B}, \quad \text{where } x = \frac{[wt \% H_2O_2]}{C}, \quad (6)$$

as proposed by Engelke *et al.* [6].

The DP reference curves are the JWL Chapman-Jouguet (CJ) isentropic release curve [7]:

$$P_{ref}(V) = A.e^{-R_1 V} + B.e^{-R_2 V} + \frac{C}{V^{\omega+1}}, \quad (7)$$

$$T_{ref}(V) = T_{CJ} \left( \frac{v_{cj}}{v} \right)^\omega. \quad (8)$$

The parameters  $A$ ,  $B$ ,  $C$ ,  $R_1$ ,  $R_2$  and  $\omega$  are determined from CHEETAH 2.0 thermochemical computation using the library NewC1 for HPS and BKWC for NM.

The shock to detonation reaction rate is a simple Arrhenius law

$$\frac{d\lambda_1}{dt} = (1 - \lambda_1) z e^{\frac{T_a}{T}}. \quad (9)$$

Its parameters for NM are well-known and available in literature [2]. For HPS, they are adjusted on plane plate impact experiment data to reproduce the characteristic times of superdetonation buildup and established detonation apparition deduced from the pyrometer measurements.

The secondary combustion reaction rate is a reduced model established from a RANS approach [1]:

$$\dot{\lambda}_2 = \frac{3D_t}{r_s^2} \log \left( \frac{0.23}{v_s} + 1 \right) (1 - \lambda_2)^{1/3}, \quad (10)$$

where  $D_t$  is the diffusion coefficient (correlation  $\rho D_t = 186 \text{ kg m}^{-1} \text{ s}^{-1}$ ),  $r_s$  the radius of the flame,  $v_s$  the stoichiometric DP-air coefficient. Computation parameters are given table 2.

**Table 2.** Parameters

	parameters	HPS	NM
Initial density	$\rho_0 \text{ (kg/m}^3\text{)}$	1290	1134
Cochran and Chan reference curve	$A_1 \text{ (GPa)}$	4.067533	0.819181
	$A_2 \text{ (GPa)}$	4.168405	1.508350
	$E_1$	3.6774	4.52969
	$E_2$	2.6774	1.42144
	$C_v$	2624	1714
	$\Gamma$	0.1	1.19
JWL reference curve	$A \text{ (GPa)}$	1110.899	218.72
	$B \text{ (GPa)}$	26.12182	6.5708
	$R_1$	6.848260	4.4
	$R_2$	2.188664	1.2
	$\omega$	0.518823	0.3
	$D_{cj} \text{ (m/s)}$	6627.33	6280.
	$P_{cj} \text{ (GPa)}$	134.1516	12.5
	$T_{cj} \text{ (K)}$	2431.33	3600.
	$C_v \text{ (J/K/kg)}$	2835.31	1900.
Arrhenius	$z \text{ (s}^{-1}\text{)}$	$2.05 \cdot 10^{13}$	$9 \cdot 10^{11}$
	$\theta \text{ (K)}$	12000.	18000.
Sound velocity proposed by Engelke <i>et al.</i> [6].	$A \text{ (m/s)}$	1488	-
	$B$	1.636	-
	$C$	105.8	-
	$D \text{ (m/s)}$	2090	-
Post-combustion	$v_s$	0.030684	0.391117
	$Q_{PostComb} \text{ (MJ/kg)}$	0.515	5.582

### 3. Results

Characteristic times of super detonation build-up and established detonation apparition deduced from the pyrometer measurements are illustrated figure 3, which represent the shock trajectory in the diagram distance-time and the luminance temperature profiles corresponding to the experiment #2. The time origin coincides with the instant the shock enters the HPS. The data provided by the pins are compared to the numerical computation of this experiment (pressure map) using the reaction rate deduced from the characteristic times.

Figure 3 illustrates the shock-to-detonation transition of HPS submitted to a 10.8 GPa plane sustained shock wave. The data provided by the pins form two lines. Their slopes, respectively, give the velocity of the initial shock and the velocity of the detonation wave. The initial shock wave velocity is well reproduced whereas the detonation one is slightly over-estimated by the numerical simulation. According to temperature measurements, it is an overdriven detonation which velocity strongly depends on the detonation product equation of state.

The numerical shock wave velocity and the temperature signals exhibit three jumps allowing to the event chronology to be identified: loading shock entrance time in HPS (time 0), formation of the superdetonation time and overtaking of the leading shock by the superdetonation, as demonstrated in the reference [2]. The time-distance chronology is well reproduced by the numerical simulation diagram shown in figure 3. The superdetonation buildup occurs at the HPS-transfer plate interface at a

speed of 11600 m/s. The induction time is defined as the delay between shock entrance and superdetonation buildup events. The depth to detonation is defined when the superdetonation overtakes the loading shock wave at 5 mm leading to an overdriven established detonation decreasing from 9000 m/s down to 7000 m/s. This overdriven detonation progressively relaxes to a stationary detonation.

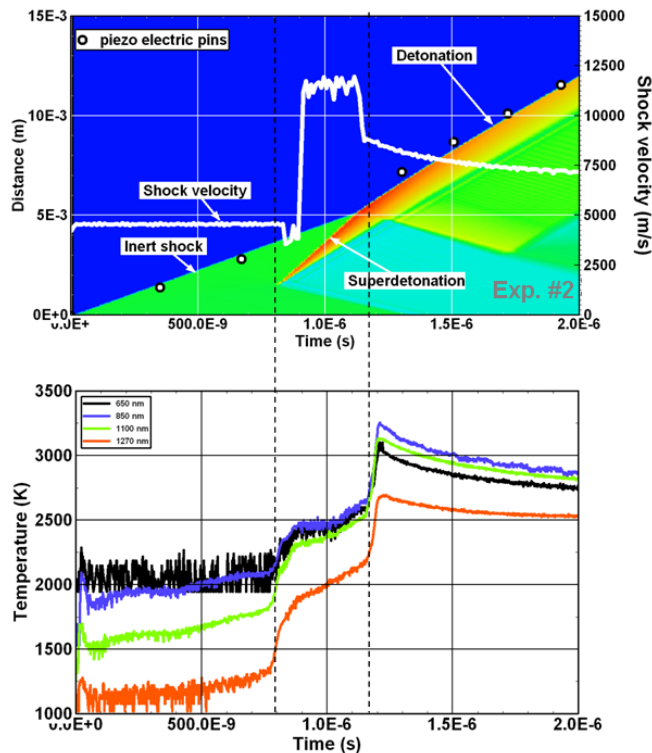


**Figure 3.** Shock to detonation transition: predicted versus experiment #2.

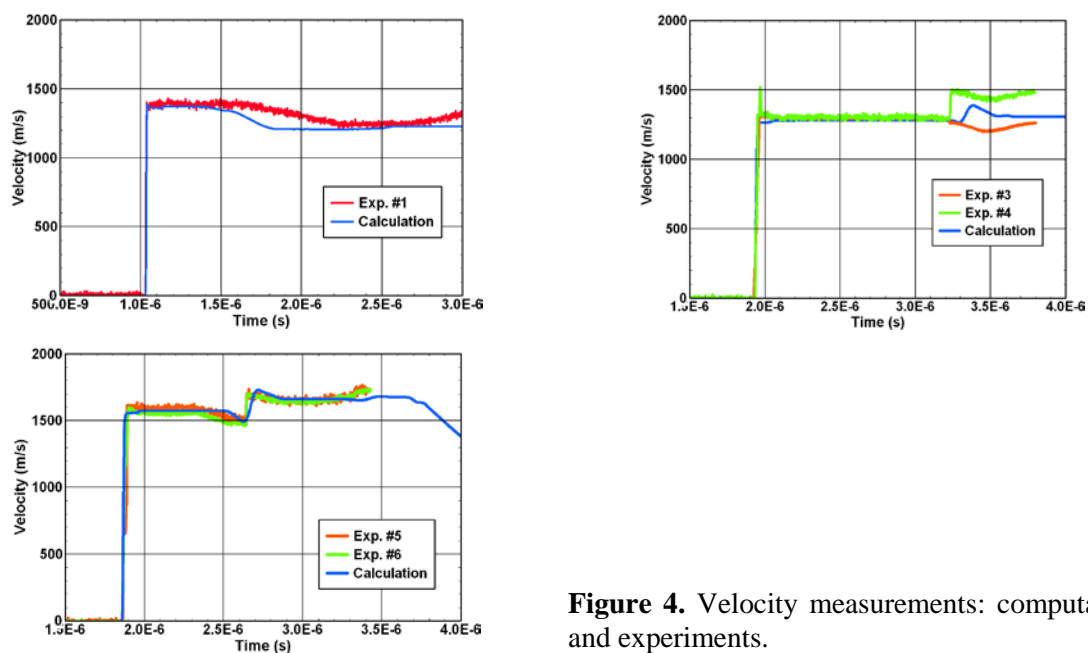


**Figure 4.** Velocity measurements: computations and experiments.

As seen in nitromethane [2], the temperatures reached prior to superdetonation buildup are too high to be consistent with the classical homogeneous model because of chemical reaction around some

heterogeneity in HPS (bubbles collapse). The superdetonation propagates in the compressed HPS by the loading shockwave and behaves as a black body at 2500 K in the 650- to 850-nm range. Behind the established detonation, the products behave as a semitransparent media in the range 2800- to 3200-K.

The back side velocities computing and recording by VISAR are plotted figure 4. Good agreement is observed between all experiment and their simulations. All velocity signals exhibit a plateau confirming a plane sustained stationary overdriven detonation.

The computed blast waves (figures 5 and 6) illustrate the effect of the oxygen balance on the fireball expansion and secondary shocks wave emerging from the fireball. These data need to be experimentally validated.

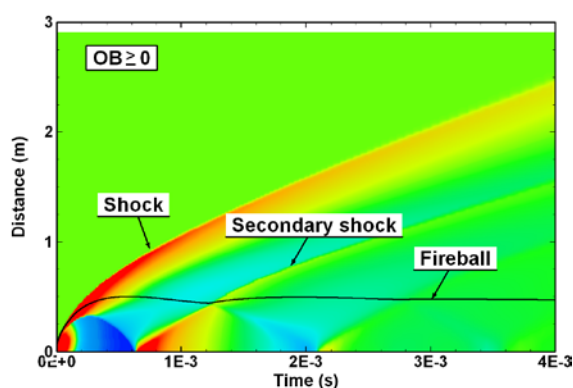


**Figure 5.** HPS computation.

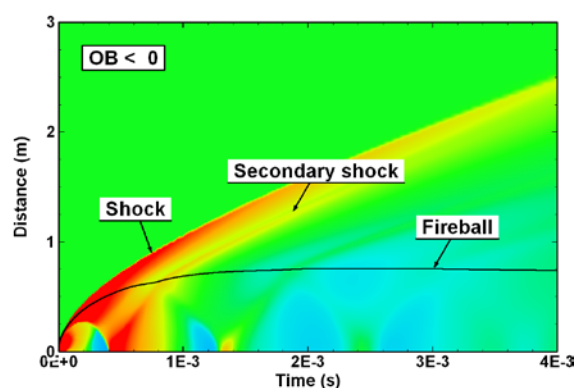


**Figure 6.** NM computation.

#### 4. Conclusion

The detonation model (equations of state and kinetic rate laws) has been validated on planar plate impact experiments realized using the ARES powder gun of caliber 98 mm. The secondary combustion parameters were deduced from thermochemical calculation. The whole model has been used to predict the effects of the oxygen balance on open air blast effects of spherical charges using an ALE 1D hydrocode. Such computations are useful for experiments design in order to validate our secondary combustion model in a wide range of oxygen balance.

#### Acknowledgments

This work has been supported by DGA of the French Ministry of Defense. Authors thank to C. Chauvin for her temperature data analysis help.

#### References

- [1] Baudin G and Munier L 2009 A simple URANS approach for secondary combustion of the detonation products *AIP Conf. Proc.* **1195** 165-8
- [2] Leal-Crouzet B, Baudin G and Presles H N 2000 Shock Initiation of Detonation in Nitromethane *Combustion and Flame* **122** 463-473
- [3] Kerley G I 1992 CTH Equation of State Package: Porosity and Reactive Burn Models *Sandia National Laboratories Tech. Rep.* SAND92-0553
- [4] Cochran S G and Chan J 1979 Shock Initiation and Detonation Models in One and Two Dimensions *Lawrence Livermore National Laboratory Tech. Rep.* UCID-18024
- [5] Woolfolk R W, Cowperthwaite M and Shaw R 1973 *Thermochimica Acta* **6** 409
- [6] Engelke R, Sheffield A S and Davis L L 2000 Experimental and Predicted Detonation Parameters for Liquid-Phase  $\text{H}_2\text{O}_2/\text{H}_2\text{O}$  Mixtures *J. Phys. Chem. A* **104** 6894-8
- [7] Lee E L, Horning H C and Kury J W 1968 Adiabatic expansion of high explosives detonation products *Lawrence Livermore National Laboratory Tech. Rep.* TID 4500-UCRL-50422